



Understanding the cytotoxic effects of new isovanillin derivatives through phospholipid Langmuir monolayers

Ana C. de Carvalho^a, Natália Girola^b, Carlos R. de Figueiredo^b, André C. Machado^a,
Lívia S. de Medeiros^a, Rafael C. Guadagnin^a, Luciano Caseli^a, Thiago A.M. Veiga^{a,*}

^a Department of Chemistry, Federal University of São Paulo, Diadema, São Paulo, Brazil

^b Department of Microbiology, Immunology and Parasitology, Experimental Oncology Unit (UNONEX), Federal University of São Paulo, São Paulo, Brazil

ARTICLE INFO

Keywords:

Cytotoxic assay
Isovanillin derivatives
Langmuir monolayers

ABSTRACT

Twenty-one isovanillin derivatives were prepared in order to evaluate their cytotoxic properties against the cancer cell lines B16F10-Nex2, HL-60, MCF-7, A2058 and HeLa. Among them, seven derivatives exhibited cytotoxic activity. We observed that for obtaining smaller IC₅₀ values and for increasing the index of selectivity, two structural features are very important when compared with isovanillin (1); a hydroxymethyl group at C-1 and the replacement of the hydroxyl group at C-3 by different alkyl groups. As the lipophilicity of the compounds was changed, we decided to investigate the interaction of the cytotoxic isovanillin derivatives on cell membrane models through Langmuir monolayers by employing the lipids DPPC (1,2-dipalmitoyl-*sn*-glycero-3-phosphocoline) and DPPS (1,2-dipalmitoyl-*sn*-glycero-3-phosphoserine). The structural changes on the scaffold of the compounds modulated the interaction with the phospholipids at the air-water interface. These results were very important to understand the biophysical aspects related to the interaction of the cytotoxic compounds with the cancer cell membranes.

1. Introduction

The structural diversity of natural products represents an important role for the development of drugs although there are still several aspects associated with them. Restrictions for discovering new drugs from specialized metabolites include metabolic instability, low solubility and low absorption in the gut to the blood preventing oral formulation [1]. For this reason, promoting structural modifications on natural products could be very useful in the search for an ideal molecule in order to increase the activity and selectivity, improving its physicochemical properties, such as solubility, distribution, ionization capacity, biochemical and/or pharmacokinetic properties [2].

Many natural compounds and their derivatives have been produced for clinical application in the treatment of several human diseases. Among these compounds, we highlight penicillin (antibacterial), morphine and benzomorphanes (analgesics), artemisinin (antimalarial), camptothecin and topotecan (anticancer). Despite the limitations presented by natural products, structural modifications may lead to the discovery of new drugs [3], and may increase the activity or efficiency against drug-resistant cells or the introduction of water-soluble groups could improve the water solubility of natural products to cross the cell membrane [3].

Artemisinin was isolated from *Artemisia annua* L [4] and presents activities against malaria [5], cancer [6] and cytomegalovirus [7]. However, the treatment of some malaria patients can be difficult due to the poor solubility in water or oil. In attempt to solve this problem some analogues were prepared in order to improve its solubility and stability [8]. One of these analogues, Artemisone, was promising and has been submitted to phase III clinical trials [9,10]. Oridonin [11], isolated from *Isodon rubescens* also had its structure modified. This compound demonstrated anticancer [12] and antibacterial activities [13]. However, the low solubility did not allow its clinical use. Alternatively, the introduction of water soluble groups increased its cytotoxicity against some cancer cell lines [10].

Plant bioactive components with amphiphilic or hydrophobic structures are cytotoxic agents, and may interact with biological and biomimetic membranes, changing their fluidity, microviscosity, elasticity and permeability [14]. Therefore, it is extremely important to investigate the interaction between compounds and the surface of cell membranes by using models, as lipid Langmuir monolayers [15,16]. This approach is based on the spreading of amphiphilic molecules at the air-liquid interface, forming a monomolecular film. When the monolayer is composed by membrane lipids spread on aqueous subphases, it

* Corresponding author.

E-mail address: tveiga@unifesp.br (T.A.M. Veiga).

<https://doi.org/10.1016/j.bioorg.2018.10.029>

Received 30 May 2018; Received in revised form 10 October 2018; Accepted 15 October 2018

Available online 19 October 2018

0045-2068/ © 2018 Elsevier Inc. All rights reserved.

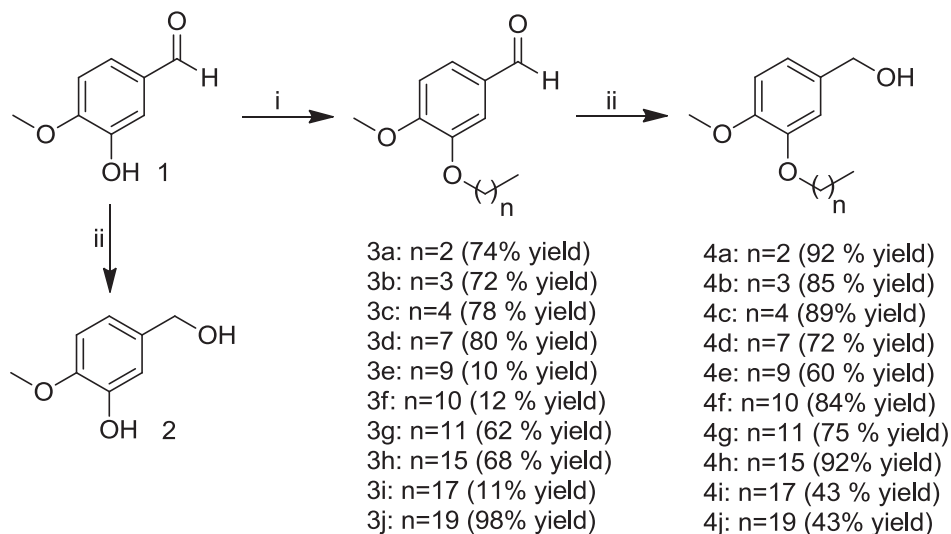
can represent a model for half-membrane, where the interface interaction between molecules can be investigated [15].

For example, the interaction of digitonin (a saponin) in lipid monolayers altered the surface pressure, surface potential and surface morphology by disturbing the lipid acyl chain orientation and the membrane fluidity [17]. Betulinic acid, α -amyrin and ursolic acid were incorporated in mitochondria lipids to understand the interaction of these triterpenes with phospholipids and correlate them with the observed anticancer activity [18]. In many cases, a biologically active natural product is an inspiration for derivatives preparations, but the main structure remains unaltered, like as: taxotere (prepared from paclitaxel) and topotecan (camptothecin's derivative) [19]. Based on this idea, we report the preparation of several derivatives from Isovanillin (1), which is a natural product found in many plant species like *Pluchea sagittalis* [20], *Pycnocycla spinosa* [21], *Mondia whitei* [22], *Benincasa hispida* [23], *Arum Palaestinum* [24], *Thalictrum przewalskii* [25], *Valeriana officinalis* var. *latifolia* [26]. Noteworthy its constitutional isomer vanillin, inhibited mutagenicity induced by chemical and physical mutagens in several models, and has chemopreventive effect in chemical carcinogenesis models, being an agent for the treatment of sickle cell anemia [27]. Moreover, it suppressed *in vitro* invasion and *in vivo* metastasis on breast cancer cells [28] as well as presented activity on human colorectal cancer cell line [29]. Vanillin derivatives also showed anticancer activity [30] against pulmonary adenocarcinoma and human leukemia cells [31]. Moreover, others Vanillin derivatives showed anticancer activity [30] against pulmonary adenocarcinoma and human leukemia cells [31].

Thus, in order to synthesize isovanillin bioactive congeners, our reactions led to the compounds 2–4j (Fig. 1). Cytotoxic activities of the derivatives were evaluated against the cancer cell lines B16F10-Nex2, HL-60, MCF-7, A2058 and HeLa. Then, we investigated the interaction of isovanillin in cell membrane models by using Langmuir monolayers. For that, selected lipids have been chosen. The lipids 1,2-dipalmitoyl-*sn*-glycero-3-phosphocoline (DPPC) and 1,2-dipalmitoyl-*sn*-glycero-3-phosphoserine (DPPS) were chosen because they represent models for tumorigenic and non-tumorigenic cells, respectively [32], since DPPS is overexpressed in tumorigenic cells [33]. Thus, we investigated the interaction of Isovanillin in cell membrane models by using lipid monolayers.

2. Experimental section

The alkyl bromides and NaBH₄ were purchased from Sigma Aldrich.



i. K₂CO₃, alkyl bromides, DMF, 5 hours; ii. NaBH₄, Ethanol, 30 minutes

Fig. 1. Scheme for preparation of the Isovanillin derivatives.

All NMR spectra were recorded on a Bruker spectrometer, Ultrashield 300 – Advance III operating at 300 MHz (¹H) and 75 MHz (¹³C). HRMS data were carried out on a Bruker Q-TOF mass spectrometer (Micro TOF-QII) equipped with an electrospray (ESI) source, operated at a resolution of 18.000 FWHM, in positive or negative mode, in the range *m/z* 100–1200. Drying gas temperature and flow was set to 200 °C and 5 L min^{−1} respectively. Capillary voltage was set to 3000 V and nozzle voltage to 500 V. The instrument was calibrated using sodium formate automatically infused prior to each analytical run and providing a mass accuracy better than 2 ppm. The samples were introduced into the MS system at 10 μL min^{−1} via an infusion pump (kdScientific).

2.1. Preparation of 3-hydroxy-4-methoxybenzenemethanol (2)

In a round-bottom flask equipped with magnetic stirrer was added sodium borohydride (0.2 mmol; 0.01 g) to the solution of 1 (0.2 mmol; 0.03 g) prepared in ethanol (1 mL). The mixture was stirred at room temperature for 30 min. The consumption of all starting material was detected by thin layer chromatography (TLC); the solvent was evaporated under reduced pressure. Subsequently, 10 mL of saturated NaCl solution was added and then extracted with ethyl acetate (3 × 10 mL). The organic phase was dried over anhydrous MgSO₄, filtered and evaporated, providing 0.03 g of colorless oil, 90% yield of 2 [34].

Compound 2. ¹H NMR (300 MHz, CDCl₃): 7.23 (dd, *J* = 7.7 and 2.8 Hz, 1H); 7.07 (d, *J* = 7.7 Hz 1H); 7.05 (d, *J* = 2.8 Hz, 1H); 4.55 (s, 2H); 3.82 (s, 3H). ¹³C NMR (300 MHz, CDCl₃): 150.6; 139.7; 133.6; 125.5; 121.8; 112.3; 64.6; 55.9.

HRMS. *m/z* 154.0615 [M+H]⁺ (calcd for C₁₁H₁₅O₃, 154.0629, Δ 9.0 ppm).

2.2. Preparation of (n)-Oxy-4-methoxybenzaldehydes (3a–3j)

In a round-bottom flask equipped with magnetic stirrer and reflux condenser was added sodium carbonate (1.97 mmol, 0.40 g) to the solution of 1 (1 mmol, 0.15 g) and dimethylformamide (DMF, 3 mL). After 10 min, the alkyl bromides (1 mmol) were added. The solutions have been kept under reflux by 5 h [35], and after determination of the consumption of all starting material by TLC, 20 mL of ethyl acetate were added, followed by the extraction with distilled water (4 × 20 mL) and saturated NaCl solution (1 × 20 mL). The organic phase was dried over MgSO₄, filtered and evaporated under reduced pressure to obtain compounds 3a–3j [35].

Compound 3a. ^1H NMR (300 MHz, CDCl_3): 9.84 (s, 1H); 7.42 (dd, $J = 8.1$ and 1.9 Hz, 1H); 7.39 (d, $J = 1.9$ Hz, 1H); 6.97 (d, $J = 8.1$ Hz, 1H); 4.03 (t, 2H); 3.95 (s, 3H); 1.89 (sext, 2H); 1.04 (t, 3H). ^{13}C NMR (75 MHz, CDCl_3): 191.0; 154.8; 149.1; 130.1; 126.6; 110.6; 110.3; 70.501; 56.2; 41.0; 22.3; 10.4.

HRMS. m/z 195.1028 $[\text{M} + \text{H}]^+$ (calcd for $\text{C}_{11}\text{H}_{15}\text{O}_3$, 195.1021, Δ 3.5 ppm).

Compound 3b. ^1H NMR (300 MHz, CDCl_3): 9.84 (s, 1H); 7.43 (dd, $J = 8.1$ and 1.9 Hz, 1H); 7.39 (d, $J = 1.9$ Hz, 1H); 6.97 (d, $J = 8.1$ Hz, 1H); 4.03 (t, 2H); 3.95 (s, 3H); 1.85 (*qui*, 2H); 1.50 (sext, 2H); 0.99 (t, 3H). ^{13}C NMR (75 MHz, CDCl_3): 191.0; 154.8; 149.2; 130.1; 126.6; 110.6; 11.2; 68.7; 56.2; 31.0; 19.2; 13.9.

HRMS. m/z 209.1176 $[\text{M} + \text{H}]^+$ (calcd for $\text{C}_{12}\text{H}_{17}\text{O}_3$, 209.1178, Δ 0.9 ppm).

Compound 3c. ^1H NMR (300 MHz, CDCl_3): 9.84 (s, 1H); 7.42 (dd, $J = 8.1$ and 1.9 Hz, 1H); 7.39 (d, $J = 1.9$ Hz, 1H); 6.97 (d, $J = 8.1$ Hz, 1H); 4.06 (t, 2H); 3.97 (s, 3H); 1.70 (*qui*, 2H); 1.50 (sext, 2H); 0.95 (t, 3H). ^{13}C NMR (75 MHz, CDCl_3): 191.0; 154.8; 149.2; 130.1; 126.6; 110.6; 110.2; 56.2; 28.7; 28.0; 22.4; 14.0.

HRMS. m/z 223.1327 $[\text{M} + \text{H}]^+$ (calcd for $\text{C}_{13}\text{H}_{19}\text{O}_3$, 223.1334, Δ 3.1 ppm).

Compound 3d. ^1H NMR (300 MHz, CDCl_3): 9.84 (s, 1H); 7.42 (dd, $J = 8.1$ and 1.9 Hz, 1H); 7.39 (d, $J = 1.9$ Hz, 1H); 6.97 (d, $J = 8.1$ Hz, 1H); 4.06 (t, 2H); 3.95 (s, 3H); 1.75 (*qui*, 2H); 1.40 (sext, 2H); 1.28 (s, 8H); 0.88 (t, 3H). ^{13}C NMR (75 MHz, CDCl_3): 191.0; 154.8; 149.2; 130.1; 126.6; 110.6; 110.2; 69.1; 56.2; 41.0; 31.8; 29.3; 29.0; 26.0; 22.6; 14.1.

HRMS. m/z 265.1799 $[\text{M} + \text{H}]^+$ (calcd for $\text{C}_{16}\text{H}_{25}\text{O}_3$, 265.1804, Δ 1.9 ppm).

Compound 3e. ^1H NMR (300 MHz, CDCl_3): 9.84 (s, 1H); 7.42 (dd, $J = 8.1$ and 1.9 Hz, 1H); 7.39 (d, $J = 1.9$ Hz, 1H); 6.97 (d, $J = 8.1$ Hz, 1H); 4.07 (t, 2H); 3.95 (s, 3H); 1.87 (sext, 2H); 1.28 (bs, 15H); 0.88 (t, 3H). ^{13}C NMR (75 MHz, CDCl_3): 191.0; 154.9; 149.2; 130.1; 126.6; 110.6; 110.3; 69.1; 56.2; 32.9; 32.00; 29.6; 29.4; 29.4; 29.1; 26.00; 22.7; 14.2.

HRMS. m/z 293.2121 $[\text{M} + \text{H}]^+$ (calcd for $\text{C}_{18}\text{H}_{29}\text{O}_3$, 293.2117 Δ 1.4 ppm).

Compound 3f. ^1H NMR (300 MHz, CDCl_3): 9.84 (s, 1H); 7.42 (dd, $J = 8.1$ and 1.9 Hz, 1H); 7.39 (d, $J = 1.9$ Hz, 1H); 6.97 (d, $J = 8.1$ Hz, 1H); 4.07 (t, 2H); 3.95 (s, 3H); 1.85 (sext, 2H); 1.28 (bs, 15H); 0.88 (t, 3H). ^{13}C NMR (75 MHz, CDCl_3): 191.0; 154.9; 149.2; 130.1; 126.6; 110.6; 110.3; 69.1; 56.2; 32.0; 29.7; 29.7; 29.6; 29.4; 29.4; 29.1; 26.0; 22.7; 14.2.

HRMS. m/z 307.2272 $[\text{M} + \text{H}]^+$ (calcd for $\text{C}_{19}\text{H}_{31}\text{O}_3$, 307.2273 Δ 0.3 ppm).

Compound 3g. ^1H NMR (300 MHz, CDCl_3): 9.84 (s, 1H); 7.42 (dd, $J = 8.1$ and 1.9 Hz, 1H); 7.39 (d, $J = 1.9$ Hz, 1H); 6.97 (d, $J = 8.1$ Hz, 1H); 4.07 (t, 2H); 3.95 (s, 3H); 1.86 (*qui*, 2H); 1.26 (bs, 18H); 0.88 (t, 3H). ^{13}C NMR (75 MHz, CDCl_3): 191.0; 154.8; 149.1; 130.0; 126.6; 110.5; 110.2; 69.0; 56.1; 31.9; 29.6; 29.6; 29.5; 29.5; 29.3; 29.3; 28.9; 25.9; 22.6; 14.1.

HRMS. m/z 321.2435 $[\text{M} + \text{H}]^+$ (calcd for $\text{C}_{20}\text{H}_{33}\text{O}_3$, 321.2430 Δ 1.5 ppm).

Compound 3h. ^1H NMR (300 MHz, CDCl_3): 9.84 (s, 1H); 7.45 (dd, $J = 8.1$ and 1.9 Hz, 1H); 7.39 (d, $J = 1.9$ Hz, 1H); 6.97 (d, $J = 8.1$ Hz, 1H); 4.07 (t, 2H); 3.95 (s, 3H); 1.86 (sext, 2H); 1.25 (bs, 26H); 0.88 (t, 3H). ^{13}C NMR (75 MHz, CDCl_3): 190.9; 154.8; 149.2; 130.1; 126.6; 110.6; 110.3; 69.1; 56.2; 31.9; 29.7; 29.6; 29.5; 29.4; 29.0; 25.9; 22.7; 14.1.

HRMS. m/z 377.3075 $[\text{M} + \text{H}]^+$ (calcd for $\text{C}_{24}\text{H}_{41}\text{O}_3$, 377.3057 Δ 4.7 ppm).

Compound 3i. ^1H NMR (300 MHz, CDCl_3): 9.83 (s, 1H); 7.45 (dd, $J = 8.1$ and 1.9 Hz, 1H); 7.39 (d, $J = 1.9$ Hz, 1H); 6.97 (d, $J = 8.1$ Hz, 1H); 4.05 (t, 2H); 3.93 (s, 3H); 1.84 (sext, 2H); 1.24 (bs, 30H); 0.86 (t, 3H). ^{13}C NMR (75 MHz, CDCl_3): 191.0; 154.9; 149.3; 130.2; 126.7; 110.6; 110.3; 69.2; 56.2; 32.0; 29.8; 29.8; 29.7; 29.7; 29.5; 29.1; 26.0;

22.8; 14.2. **HRMS.** m/z 405.3349 $[\text{M} + \text{H}]^+$ (calcd for $\text{C}_{26}\text{H}_{45}\text{O}_3$, 405.3369 Δ 4.9 ppm).

Compound 3j. ^1H NMR (300 MHz, CDCl_3): 9.84 (s, 1H); 7.42 (dd, $J = 8.1$ and 1.9 Hz, 1H); 7.39 (d, $J = 1.9$ Hz, 1H); 6.97 (d, $J = 8.1$ Hz, 1H); 4.06 (t, 2H); 3.95 (s, 3H); 1.80 (sext, 2H); 1.26 (bs, 34H); 0.87 (t, 3H). ^{13}C NMR (75 MHz, CDCl_3): 191.0; 154.8; 149.2; 130.1; 126.6; 110.5; 110.2; 69.1; 56.1; 31.9; 29.7; 29.4; 29.00; 25.9; 22.7; 14.1.

HRMS. m/z 455.3490 $[\text{M} + \text{Na}]^+$ (calcd for $\text{C}_{28}\text{H}_{48}\text{O}_3\text{Na}$, 455.3501 Δ 2.4 ppm).

2.3. Preparation of Oxy-4-methoxybenzenemethanols (4a – 4j)

In a round-bottom flask with magnetic stirrer was added sodium borohydride (NaBH_4) and the alkylated derivatives (3a – 3j) in dichloromethane (DCM, 1 mL) or ethanol (EtOH, 1 mL) solution. The solutions were stirred at room temperature for 30 min [34]. After depletion of the starting material, the solvent was removed under reduced pressure. Thereafter, saturated NaCl solution (10 mL) was added and the extraction with ethyl acetate (3×10 mL) has been done. The organic phase was dried over anhydrous MgSO_4 , filtered and evaporated under reduced pressure producing yellowish solids with on average of 98% yield [34].

Compound 4a. ^1H NMR (300 MHz, CDCl_3): δ 6.92 (dd, $J = 10.9$ and 1.7 Hz, 1H); 6.87 (d, $J = 1.7$ Hz, 1H); 6.85 (d, $J = 8.1$ Hz, 1H); 4.55 (bs, 2H); 3.95 (t, 2H); 3.83 (s, 3H); 1.84 (sext, 2H); 1.02 (t, 3H). ^{13}C NMR (75 MHz, CDCl_3): δ 148.6; 133.7; 119.37; 112.14; 111.6; 70.3; 65.1; 56.1; 22.5; 10.4.

HRMS. m/z 219.1003 $[\text{M} + \text{Na}]^+$ (calcd for $\text{C}_{11}\text{H}_{16}\text{O}_3\text{Na}$, 219.0997 Δ 2.7 ppm).

Compound 4b. ^1H NMR (300 MHz, CDCl_3): δ 6.92 (dd, $J = 8.8$ and 1.5 Hz, 1H); 6.87 (d, $J = 1.8$ Hz, 1H); 6.85 (d, $J = 8.1$ Hz, 1H); 4.61 (bs, 2H); 4.03 (t, 2H); 3.49 (s, 3H); 1.84 (sext, 2H); 0.98 (t, 3H). ^{13}C NMR: δ 149.0; 148.7; 130.8; 120.3; 112.8; 111.4; 71.7; 68.7; 56.1; 31.3; 19.2; 13.9

HRMS. 233.1157 m/z 233.1003 $[\text{M} + \text{Na}]^+$ (calcd for $\text{C}_{12}\text{H}_{18}\text{O}_3\text{Na}$, 233.1154 Δ 1.8 ppm).

Compound 4c. ^1H NMR (300 MHz, CDCl_3): δ 6.92 (dd, $J = 10.8$ and 1.4 Hz, 1H); 6.87 (d, $J = 1.7$ Hz, 1H); 6.85 (d, $J = 8.1$ Hz, 1H); 4.59 (bs, 2H); 4.00 (t, 2H); 3.84 (s, 3H); 2.03 (s, OH); 1.84 (*qui*, 2H); 1.34 (sext, 2H); 0.92 (t, 3H). ^{13}C NMR (75 MHz, CDCl_3): δ 149.0; 148.6; 130.8; 120.4; 112.8; 111.4; 71.7; 69.0; 56.1; 28.9; 28.1; 22.5 14.0 **HRMS.** m/z 247.1296 1324 $[\text{M} + \text{Na}]^+$ (calcd for $\text{C}_{12}\text{H}_{18}\text{O}_3\text{Na}$, 247.1310 Δ 5.6 ppm).

Compound 4d. ^1H NMR (300 MHz, CDCl_3): δ 6.92 (dd, $J = 10.5$ and 1.3 Hz, 1H); 6.87 (d, $J = 1.6$ Hz, 1H); 6.85 (d, $J = 8.1$ Hz, 1H); 4.55 (bs, 2H); 3.97 (t, 2H); 3.81 (s, 3H); 1.80 (sext, 2H); 1.25 (bs, 10H) 0.85 (t, 3H). ^{13}C NMR (75 MHz, CDCl_3): δ 148.4; 148.2; 133.8; 119.1; 112.0; 111.4; 68.8; 55.7; 31.4; 29.1; 25.7; 22.4; 13.7.

HRMS. m/z 289.1782 $[\text{M} + \text{Na}]^+$ (calcd for $\text{C}_{16}\text{H}_{26}\text{O}_3\text{Na}$, 289.1779 Δ 1.0 ppm).

Compound 4e. ^1H NMR (300 MHz, CDCl_3): δ 6.92 (dd, $J = 9.7$ and 1.3 Hz, 1H); 6.87 (d, $J = 1.6$ Hz, 1H); 6.85 (d, $J = 8.1$ Hz, 1H); 4.58 (bs, 2H); 3.99 (t, 2H); 3.84 (s, 3H); 1.83 (sext, 2H); 1.26 (bs, 7H) 0.87 (t, 3H). ^{13}C NMR (75 MHz, CDCl_3): δ 149.1; 148.8; 133.7; 119.4; 112.2; 111.6; 69.1; 65.4; 56.2; 32.0; 29.7; 29.5; 29.4; 29.3; 26.1; 22.8; 14.2.

HRMS. m/z 317.2079 $[\text{M} + \text{Na}]^+$ (calcd for $\text{C}_{18}\text{H}_{30}\text{O}_3\text{Na}$, 317.2092 Δ 0.6 ppm).

Compound 4f. ^1H NMR (300 MHz, CDCl_3): δ 6.92 (dd, $J = 9.6$ and 1.4 Hz, 1H); 6.87 (d, $J = 1.7$ Hz, 1H); 6.85 (d, $J = 8.1$ Hz, 1H); 4.55 (bs, 2H); 3.97 (t, 2H); 3.82 (s, 3H); 1.82 (sext, 2H); 1.26 (bs, 10H); 0.87 (t, 3H). ^{13}C NMR (75 MHz, CDCl_3): δ 148.9; 133.8; 119.3; 112.1; 111.5; 69.1; 65.1; 56.0; 31.9; 29.5; 29.4; 26.0; 22.7; 14.1.

HRMS. m/z 331.2247 $[\text{M} + \text{Na}]^+$ (calcd for $\text{C}_{19}\text{H}_{32}\text{O}_3\text{Na}$, 331.2249 Δ 0.6 ppm).

Compound 4g. ^1H NMR (300 MHz, CDCl_3): δ 6.92 (dd, $J = 7.2$ and 1.6 Hz, 1H); 6.87 (d, $J = 1.6$ Hz, 1H); 6.85 (d, $J = 8.1$ Hz, 1H); 4.54

(bs, 2H); 3.97 (t, 2H); 3.82 (s, 3H); 1.82 (sext, 2H); 1.26 (bs, 10H) 0.87 (t, 3H). ^{13}C NMR (75 MHz, CDCl_3): δ 149.1; 148.9; 133.7; 119.5; 112.2; 111.7; 69.2; 65.5; 56.2; 32.1; 29.7; 29.5; 29.3; 26.1; 22.8; 14.2. HRMS. m/z 345.2400 $[\text{M} + \text{Na}]^+$ (calcd for $\text{C}_{20}\text{H}_{34}\text{O}_3\text{Na}$, 345.2406 Δ 1.7 ppm)

Compound 4h. ^1H NMR (300 MHz, CDCl_3): δ 6.92 (dd, J = 7.2 and 1.6 Hz, 1H); 6.87 (d, J = 1.7 Hz, 1H); 6.85 (d, J = 8.1 Hz, 1H); 4.60 (d, J = 5.8 Hz, 2H); 4.00 (t, 2H); 3.85 (s, 3H); 1.84 (sext, 2H); 1.25 (bs, 26H); 0.88 (t, 3H). ^{13}C NMR (75 MHz, CDCl_3): δ 149.0; 133.5; 119.3; 120.0; 111.3; 69.0; 65.3; 56.1; 31.9; 29.7; 29.4; 29.2; 26.0; 22.7; 14.1.

HRMS. m/z 401.3001 $[\text{M} + \text{Na}]^+$ (calcd for $\text{C}_{24}\text{H}_{42}\text{O}_3\text{Na}$, 401.3032 Δ 7.7 ppm)

Compound 4i. ^1H NMR (300 MHz, CDCl_3): δ 6.92 (dd, J = 9.7 and 1.6 Hz, 1H); 6.87 (d, J = 1.6 Hz, 1H); 6.85 (d, J = 8.1 Hz, 1H); 4.58 (d, J = 5.8 Hz, 2H); 4.00 (t, 2H); 3.84 (s, 3H); 1.82 (sext, 2H); 1.25 (s, 14); 0.87 (t, 3H). ^{13}C NMR (75 MHz, CDCl_3): δ 149.1; 148.8; 133.7; 119.5; 112.2; 111.7; 69.1; 65.4; 56.2; 32.1; 29.8; 29.7; 29.7; 29.5; 29.5; 29.3; 26.1; 22.8; 14.2.

HRMS. m/z 429.3358 $[\text{M} + \text{Na}]^+$ (calcd for $\text{C}_{20}\text{H}_{34}\text{O}_3\text{Na}$, 429.3345 Δ 3 ppm)

Compound 4j. ^1H NMR (300 MHz, CDCl_3): δ 6.92 (dd, J = 9.5 and 1.5 Hz, 1H); 6.87 (d, J = 1.6 Hz, 1H); 6.85 (d, J = 8.1 Hz, 1H); 4.61 (d, J = 5.8 Hz, 2H); 4.02 (t, 2H); 3.86 (s, 3H); 1.83 (sext, 2H); 1.25 (bs, 34H); 0.88 (t, 3H). ^{13}C NMR (75 MHz, CDCl_3): δ 119.2; 118.9; 133.7; 119.5; 112.2; 111.7; 69.2; 65.5; 56.2; 32.1; 26.1; 22.8; 14.3.

HRMS. 457.3637 m/z 457.358 $[\text{M} + \text{Na}]^+$ (calcd for $\text{C}_{20}\text{H}_{34}\text{O}_3\text{Na}$, 457.3658 Δ 4.5 ppm).

2.4. Tumor cells and culture conditions

The murine melanoma cells B16F10 were originally obtained from the Ludwig Institute for Cancer Research (LICR), São Paulo Branch. The lineage B16F10-Nex2 was isolated at the Experimental Oncology Unit (UNONEX) from the Federal University of São Paulo (UNIFESP) and registered in the *Banco de Células do Rio de Janeiro* (BCRJ), N° 0342. Human melanoma cell lines (A2058), breast adenocarcinoma (MCF-7), uterine cervix adenocarcinoma (HeLa) and promyelocytic leukemia (HL-60) have been provided by the LICR. Both cell lines were cultivated in culture bottles, using RPMI 1640 (Gibco, Grand Island, NY) supplemented with 10 mM of N-(2-hydroxyethyl)-piperazine-N'-2-ethanesulfonic acid (HEPES; Sigma-Aldrich, St. Louis, MO), 24 mM of sodium bicarbonate, 40 mg L^{-1} of Gentamicin (Hipolabor, Minas Gerais, Brazil) at pH 7.2, and 10% of fetal bovine serum (Invitrogen). Cells were cultivated at 37 °C in a humidified atmosphere and 5% of CO_2 .

2.5. In vitro cytotoxic assay

To estimate the IC_{50} values, 1×10^4 of tumor cell lines were seeded in 96-well plates and treated with different concentrations of each compound ranging from 0 to 100 $\mu\text{g mL}^{-1}$ for 24 h. Viable cells were quantified by colorimetric assay, using MTT (3-[4,5-dimethylthiazol-2-yl]-2,5-diphenyltetrazolium bromide) (Sigma-Aldrich, St. Louis, MO). After incubation, 10 μL of MTT solution (5 mg mL^{-1}) was added to the cells, followed by incubation for 3 h at 37 °C. Then, a solution of 10% of sodium dodecyl sulfate (Sigma-Aldrich, St. Louis, MO) was added to each well. The absorbance was measured with a spectrophotometric automated plate reader (SpectraMax-M2, Molecular Devices, Sunnyvale, CA) at 570 nm. IC_{50} was measured using GraFit 5 data analysis software (Version 5.0.13).

2.6. Langmuir monolayers

The lipids DPPC and DPPS were purchased from Sigma-Aldrich and solubilized in chloroform (Synth) to prepare a 0.5 mg mL^{-1} solution. Water was purified from a Milli-Q system (resistivity 18.2 $\text{M}\Omega\text{-cm}$). The Langmuir monolayers were then obtained by spreading an aliquot of

lipid solutions on the air-water interface of water contained in a Langmuir trough (KSV – model mini) made of Teflon® and equipped with surface pressure sensor and a polarization modulation infrared reflection-absorption spectrometer (PM-IRRAS) obtained from KSV (PMI 550 instrument).

For preliminary tests, derivatives **3e**, **3f**, **3g**, **4e**, **4f**, **4g** and **4h**, solubilized in chloroform to a final concentration of 0.5 mg mL^{-1} , were spread individually on the air-water interface in order to test their surface activity. For mixed Isovannillin-lipid monolayers, both compounds were co-spread at the air-water interface with selected proportions. After 30 min for chloroform evaporation and homogenization, surface pressure-area (π -A) isotherms were obtained by compressing the monolayer at a rate of 5 $\text{\AA}^2 \text{ molecule}^{-1} \text{ min}^{-1}$. All experiments were carried out at a controlled room temperature (300 K) and conducted at least three times to test the reproducibility.

3. Results and discussion

Isovannillin structural modifications have been performed in order to change some functional groups, but keeping the main scaffold to verify if the variations could increase the cytotoxic activity that was not observed for compound **1**. Firstly the aldehyde carbonyl was replaced by an oxymethylene group to obtain compound **2**. This compound also did not present activity against tested cancer cell lines, B16F10-Nex2, HL-60, MCF-7, A2058 and HeLa. Due to this fact, we have decided to observe if the replacement of the hydroxyl group (position C-3) by an alkyl chain with a variable number of methylene groups could turn the compound more lipophilic, and consequently more active.

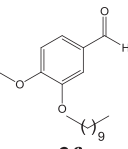
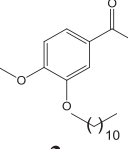
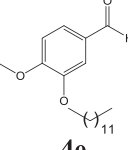
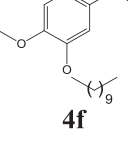
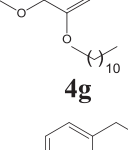
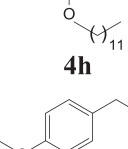
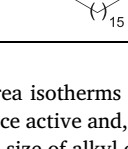
In this way, in order to investigate the relationship between the length of the alkyl chain and the cytotoxic effects, derivatives **3a** – **3j** were prepared with alkyl chains of 3, 4, 5, 8, 10, 11, 12, 16, 18 and 20 carbons at C-3 along with carbonyl group at C-1. Compounds **3e** and **3f** presented activity against B16F10-Nex2, HL-60, MCF-7, A2058 and HeLa. In its turn, derivative **3g** also presented activity against all of them, except for MCF-7 (Table 1).

Due to the activity of the compounds **3e**, **3f**, **3g** we have decided to prepare their derivatives originating compounds **4e**, **4f** and **4g**. Thus, they were obtained with a hydroxymethylene group at C-1 obtained by using NaBH_4 as reducing agent. Compounds **4e**, **4f** and **4g** presented smaller IC_{50} values (Table 1) than their related aldehydes. Thus, to investigate if the merger between both structural features is responsible for maintaining the activity, we also prepared the derivatives **4a**, **4b**, **4c**, **4d**, **4h**, **4i** and **4j** from compounds **3a**, **3b**, **3c**, **3d**, **3h**, **3i** and **3j**, respectively.

Initially, the analysis of the IC_{50} values (Table 1) suggested the importance of the structural features for increasing the cytotoxic activity: the alkyl chain from 10 to 17 carbons and the hydroxymethylene group at C-1. Derivatives **3e**, **3f**, **3g**, **4e**, **4f**, **4g** and **4h** presented cytotoxicity against cell lines B16F10-Nex2, HL-60, MCF-7, A2058, HeLa, except **3g** and **4g** that did not present effect against MCF-7 (Table 1). Compound **4g** showed higher cytotoxicity and index of selectivity (I.S.) than others against cell lines B16F10-Nex2 ($\text{IC}_{50} = 30.4 \pm 4.6$; I.S. = 3.04), HL-60 ($\text{IC}_{50} = 26.4 \pm 1.3$; I.S. = 3.78), A2058 ($\text{IC}_{50} = 19.8 \pm 3.0$; I.S. = 5.04) and HeLa ($\text{IC}_{50} = 18.8 \pm 1.1$; I.S. = 5.30) (Table 1). In comparison, its precursor **3g** which presented IC_{50} values bigger than **4g**. However, in this specific case, we observed that the hydroxyl group caused a decrease on IC_{50} and an increase of the I.S., that is a very important aspect in cytotoxic studies. All compounds, except **3g** and **4g** presented activity against MCF-7. This cell line is deficient in caspase-3 [36]. Caspase-3 is a protein which is directly related to a cell death by apoptosis [37]. If the compound presented the activity against MCF-7, there are indications that the mechanism of action is not by induction of apoptosis via caspase-3 [38].

To understand and suggest how the active compounds interact with membrane models, pure isovannillin derivatives were spread on the air-water interface, and compressed in order to obtain surface pressure-

Table 1
Calculated IC₅₀ (μg mL⁻¹) values and index of selectivity (I.S.) for the assayed isovanillin derivatives.

Compounds	Cell lines				
	B16F10-Nex2	HL-60	MCF-7	A2058	HeLa
3e 	I.S. = 1.06 IC ₅₀ = 53.9 ± 2.4	I.S. = 2.24 IC ₅₀ = 25.4 ± 0.4	I.S. = 1.71 IC ₅₀ = 32.8 ± 1.7	I.S. = 1.14 IC ₅₀ = 49.9 ± 1.7	I.S. = 0.67 IC ₅₀ = 85 ± 3.1
3f 	I.S. = 1.51 IC ₅₀ = 30.8 ± 1.3	I.S. = 2.02 IC ₅₀ = 23.1 ± 1.3	I.S. = 2.60 IC ₅₀ = 17.9 ± 0.3	I.S. = 1.65 IC ₅₀ = 28.2 ± 0.9	I.S. = 1.9 IC ₅₀ = 24.4 ± 0.7
3g 	I.S. = 0.70 IC ₅₀ = 66.0 ± 1.7	I.S. = 0.75 IC ₅₀ = 52 ± 1.5	I.S. = 0.71 IC ₅₀ > 100	I.S. = 1.17 IC ₅₀ = 68 ± 0.01	I.S. = 0.72 IC ₅₀ = 93 ± 2.4
4e 	I.S. = 1.43 IC ₅₀ = 24.9 ± 0.5	I.S. = 2.68 IC ₅₀ = 13.3 ± 1.0	I.S. = 2.24 IC ₅₀ = 15.9 ± 0.1	I.S. = 1.64 IC ₅₀ = 21.8 ± 1.6	I.S. = 1.56 IC ₅₀ = 22.8 ± 1.4
4f 	I.S. = 1.33 IC ₅₀ = 28.1 ± 0.6	I.S. = 2.29 IC ₅₀ = 16.3 ± 0.8	I.S. = 1.62 IC ₅₀ = 23.0 ± 0.4	I.S. = 1.57 IC ₅₀ = 23.8 ± 0.5	I.S. = 1.46 IC ₅₀ = 25.5 ± 1.3
4g 	I.S. = 3.04 IC ₅₀ = 30.4 ± 4.6	I.S. = 3.78 IC ₅₀ = 26.4 ± 1.3	I.S. = 0.99 IC ₅₀ > 100	I.S. = 5.04 IC ₅₀ = 19.8 ± 3.0	I.S. = 5.30 IC ₅₀ = 18.8 ± 1.1
4h 	I.S. = 1.07 IC ₅₀ = 73.0 ± 0.9	I.S. = 1.36 IC ₅₀ = 72.0 ± 1.3	I.S. = 1.14 IC ₅₀ = 47.0 ± 2	I.S. = 1.04 IC ₅₀ = 46.0 ± 0.9	I.S. = 0.76 IC ₅₀ = 54.0 ± 7.2

area isotherms (Fig. 2). The isotherms have showed that they are surface active and, except for the compounds **3e** and **4e**, which are smaller in size of alkyl chain, are able to increase the surface pressure to values above zero. This high increase of surface pressure, even in relative large molecular areas, can indicate an aggregation behavior. The minimum areas attained before collapse for the major of the case were below 30 Å², which is compatible with their approximate sizes. Particularly, for the compounds **3f** – **3h**, which contain carbonyl at C-1, the general profile of the curve is a smooth increase of the surface pressure upon compression until a plateau is attained at 10, 13 and 30 mN/m, respectively. At the plateau is probably that the collapse has been attained, although for the compound **3f** a sequential increase of surface pressure is observed after this plateau up to 20 mN/m. The relative values of surface pressure are compatible with their size of chain, i.e., longer chain leads to higher surface activities.

For the compounds **4e** to **4h**, which contain a hydroxymethylene group at C-1, the profile of the isotherm for the compound **4e** does not change considerably in comparison with the previous group in **3e**. However, for the compounds **4f**, **4g**, and **4h** the initial surface pressure is initially higher and further compression leads to progressive increase of the surface pressure with an indefinite collapse. It is probable therefore that the variation of the polar group may change the rheological properties of the monolayer and also the dissipation of energy when the film is mechanically compressed.

Although we have performed mixtures of DPPC with a larger number of compounds (as shown later in Fig. 4), we decided to focus in the effect of three of them to easy the physical chemical interpretation as shown in Fig. 3. Panel A shows the surface pressure-area isotherms for DPPC monolayers. The pure DPPC monolayer presents a typical curve, collapsing at 50 Å²/molecule and a typical plateau around 12

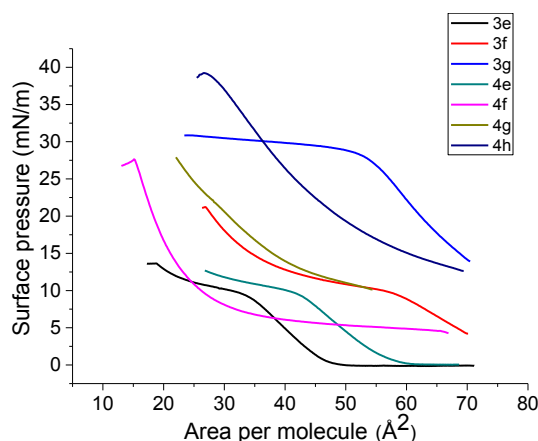


Fig. 2. Surface pressure-area isotherms for the isovanillin derivatives.

mN/m, representing the transition between the liquid-expanded (LE) and liquid-condensed (LC) phases. The introduction of these compounds in the monolayer shifts the isotherm to higher molecular areas of DPPC at low surface pressure values, indicating the penetration of the compound in the lipid monolayer. However at high surface pressures, attained when the film is compressed to lower areas, the compounds seem to be expelled from the monolayer since the areas for the mixed films are lower than from pure DPPC. It is important to highlight that the molecular areas shown in the x-axis is attributed only for DPPC and not for the other treatments (DPPC + isovanillin derivatives). This was done in order to compare the effect of small amounts of isovanillin derivatives onto the DPPC monolayer.

For compound **3g**, interestingly, we observe a second plateau around 30 mN/m, which may represent the phase where the compound is being expelled from the interface. For compound **4g**, particularly, the effect is more evident as it causes an instantly raise in the surface pressure even at high molecular areas. Further compression leads the monolayer to a plateau at 40 mN/m and a sequential raise of the surface pressure at very low areas (30 Å²). This plateau may present not only the mechanism for expelling the compounds from the monolayer, but also the disruption of the film monomolecular structure. Possibly **4g** destroys the film, taking together some DPPC molecules to the collapse structure since the area of 30 Å² is too low considering the structure of the lipid. This may be related to the cytotoxic effect observed for **4g**.

Fig. 3B shows the surface elasticity (*E*) of the monolayers, defined as $-A(\partial\pi/\partial A)T$ (*A*: molecular area; π : surface pressure; *T*: temperature). At about 12 mN/m, the decrease of the *E* values is related to the LE-LC transition. The plateaus for **3g** and **4g** observed in their surface pressure-area isotherm at 30 and 40 mN/m, respectively, can be observed in the elasticity curves by the low values of *E* in the correspondent curves

and values of surface pressure. The mixtures of DPPC with all compounds presented maximum high values *E* (about 200 mN/m), featuring the LC state. This value may represent mainly the effect of DPPC, which alone also attains high values of *E* relatively (250 mN/m). However, the decrease from 250 mN/m (pure DPPC) to 200 mN/m (mixed monolayers) could be attributed to the effect of the isovanillin derivatives disturbing the rheological properties of the film. Although at this stage, the derivatives may be expelled from the interface, they must be located nearby of the film since they are lipophilic and aqueous insoluble. Therefore, such interaction may still affect the values of surface elasticity of the film because of viscoelastic effects.

In Fig. 4, we showed once more the effect of the compounds **3g**, **4g** and **4h**; beyond that we observed the effect of all other compounds investigated. We believe in this way we can better correlate the similarity between the structures with the similarity between the isotherm profiles. Broadly speaking, the compound **3e** presented a similar isotherm profile to the isotherm generated by **3g**. However, the collapse was achieved at lower values of surface pressure. Furthermore, the compounds **4e** and **4f** presented similar profile than **4g**. Compound **3f**, however, present a very specific isotherm when mixed with DPPC, presenting a high surface activity, even at high film areas, and the curve presents an expanded monolayer in relation to the pure lipid monolayer, indicating that the compound has not been expelled from the film. These features, in general, are also observed in the elasticity curves (Fig. 4B).

The compounds **3e** and **3g** present a difference of only 2 methylene groups in the alkyl chain at C-3, but **3f**, even present a alkyl chain with an intermediate size between **3e** and **3g**, it presents a more expanded monolayer, indicating that a single addition of a methylene group in the alkyl chain of the compound affected the surface activity properties on the DPPC monolayer. However the profile of the isotherm is similar even comparing **3f** with **3e** and **3g**, and the main difference is on the occupancy area. It is probably that **3f** may be arranged molecularly with DPPC at the air-water interface at such a way that either provides repulsion among the chains, or the mixed monolayer component may suffer geometrical restrictions to accommodate at the interface. Furthermore, the compounds **4e**, **4f** and **4g** also present differences only in the size of the alkyl group (with 9, 10, and 11 methylene groups, respectively). Compound **4h** is also similar to these compounds, but this distinctive isotherm can be explained by the higher number of methylene groups (15). Curiously, it is the compound with size more comparable to that for DPPC, and it presents the isotherm with a profile more similar to that for pure DPPC. This point leads us to an important finding: that compounds with similar alkyl chain sizes may adapt better at the air-water interface, causing less effect regarding 2D-transitions, expelling from the interface, and collapse process. It likely, therefore, that the compound **4h** and DPPC may be molecularly arranged as a mixed Langmuir monolayer that can be packed regularly when laterally compressed.

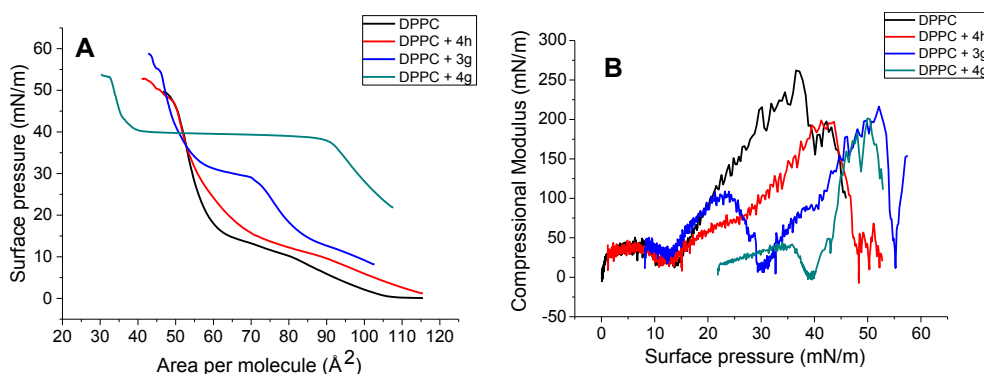


Fig. 3. Surface pressure-area (A) and compressional modulus-surface pressure (B) isotherms for DPPC, pure or mixed with the compounds **3g**, **4g** and **4h** (5% in mol).

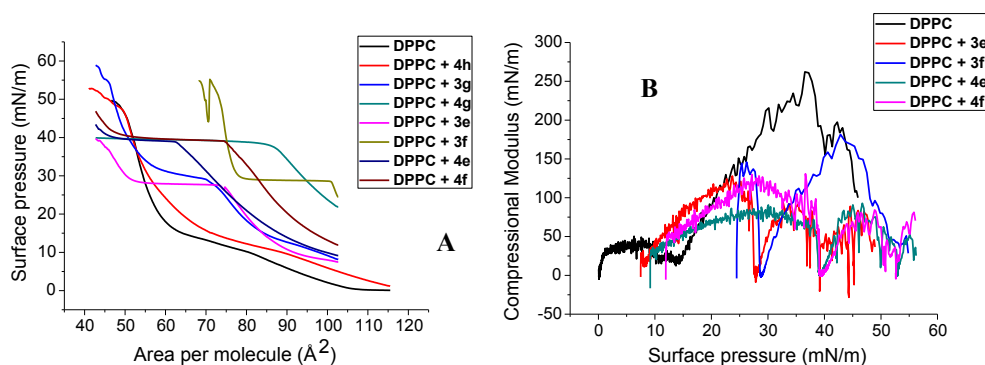


Fig. 4. Surface pressure-area (A) and compressional modulus-surface pressure (B) isotherms for DPPC, pure or mixed with the isovanillin derivatives (5% in mol) and indicated in the inserts.

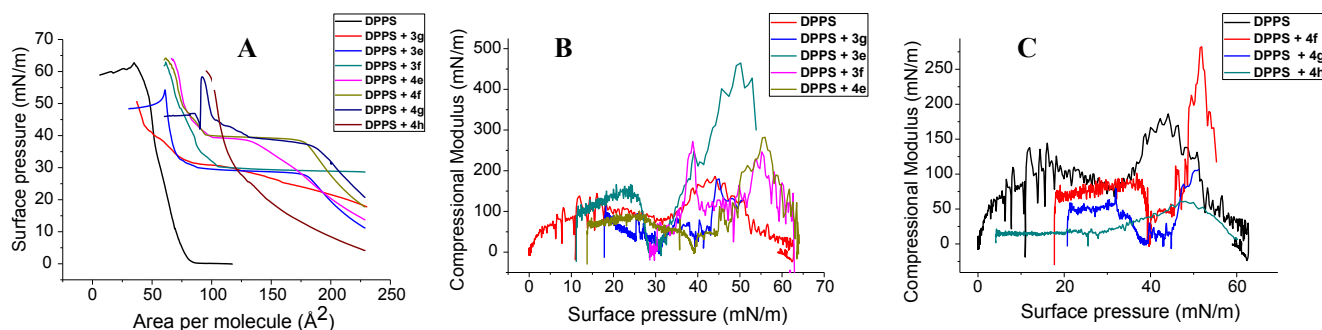


Fig. 5. Surface pressure-area (A) and compressional modulus-surface pressure (B and C) isotherms for DPPS, pure or mixed with the isovanillin derivatives (5% in mol) and indicated in the inserts.

Fig. 5 shows the effect of the same compounds with DPPS, a lipid encountered in high quantities in tumorigenic cells [33]. Curiously, except for the compound **3g**, all other tested compounds expanded the lipid monolayer, which contrast with the effect on DPPC monolayers, once the condensation of the monolayer presented the behavior more commonly encountered. The profiles of the isotherms are almost all similar, generally speaking. There is an initial increase of the surface pressure at high molecular areas, with compression it is attained a plateau at high surface pressures (30 or 40 mN/m), and after sequential compression, the pressure raises again and the monolayer collapses. Interestingly the compounds **3e**, **3f** and **3g** present all a plateau at 30 mN/m, and they differs only in the number of methylene groups on the alkyl chain. In its turn, compounds **4e**, **4f** and **4g** presented a plateau at 40 mN/m and also only differ on the size of the alkyl chain, but with an hydroxymethylene group at C-1. It can be conclude, therefore, that the chemical differential of the two set of compounds (the presence of a carbonyl or a hydroxyl group) is the factor that determines the surface pressure of this plateau. Consistently, the compound **4h** was the only one that did not present such plateau, showing a isotherm only more expanded (shifted to higher areas) and more compressible than DPPS (presented lower values of elasticity as shown in Panel 5C, and also clear observing the inclination of the surface pressure-area isotherms). In this case, the explanation is similar to that for DPPC. The similarity between the size of the derivative and the phospholipid may determine a better molecular accommodation at the air-water interface when the lipid-derivative is packed due to the lateral compression.

Although the correlation of the surface properties of each compound with their cytotoxic properties presented in Table 1 is not straightforward, we can steadfastly conclude that the small changes in the chemical structure of the compounds not only alter the cytotoxicity activities on several selected cell lines, but also they modulate the interaction with the phospholipid at the air-water interface. This interaction is highly dependent on the chemical structure of the lipid, since for DPPS, a negative charged lipid and a model for tumorigenic

cells, the incorporation of small amounts of the compound basically expanded the monolayers, whereas for DPPC, a zwitterionic charged lipid and model for non-tumorigenic cells, it condenses the monolayers. Such distinctive interaction may be resulted from different electrostatic interactions between the compounds and the lipid concerning not only interactions between net charges, but also between polar and apolar regions.

For the myriad of seven lipids employed in this work, compound **4h**, particularly, presented a less characteristic effect on the monolayer isotherms, and we believe that it must be related to the similar size of this compound to lipids employed. For the other derivatives, we can separate them in two groups since those with hydroxyl and those with carbonyl groups presented distinctive behavior in terms of 2D phase transition concerning the surface pressure-area isotherms.

By employing lipid monolayers was possible to understand the cytotoxic activities of isovanillin derivatives. This approach is becoming an interesting tool to go further on chemistry of interfaces. In the analyses of natural products, some studies have used similar methods for different biological targets. Broniatowski et al. [39], evaluated the antibacterial activity of some pentacyclic triterpenes. As the model membrane, were applied mixtures of the representative *Escherichia coli* phosphatidylethanolamine (POPE), with the cardiolipin (ECCL) or phosphatidylglycerol (ECPG) extracted from the *E. coli* inner membrane. Violacein, a bis-indole pigment, was investigated on cell membrane models represented by selected lipids, dipalmitoylphosphatidylcholine/DPPC (healthy cellular membranes), and dipalmitoylphosphatidylserine/DPPS (tumorigenic cellular membranes). Morphological analysis also suggests that violacein at the air-water interface is homogenized when incorporated in both lipids [32]. These results therefore may have important implications in understanding how violacein acts on specific sites of the cellular membrane, and evidence the fact that the lipid composition of the monolayer modulates the interaction with the lipophilic drug.

Similar study was performed for Quercetin. The flavonoid

incorporation diminishes the monolayer surface elasticity for DPPC and causes a relative decrease of the intensity for C–H stretch bands, pointing to a disruption of the packed order of DPPC. These results can be associated to the interaction between Quercetin and cell membrane surfaces during biochemical processes, which may influence its pharmaceutical properties [15]. A higher monolayer expansion was observed for DPPS and DODAB in the presence of Eugenol [40]. These results pointed to the fact that the interaction of Eugenol with lipid monolayers at the air–water interface is modulated by the lipid composition, which may be important to comprehend at the molecular level the interaction of this drug with biological surfaces.

4. Conclusion

Our results suggest that is possible to highlight new insights about the interaction of cytotoxic natural products derivatives over cell membrane components. Parameters corresponding to the intermolecular interactions and their effects on the thermodynamic and rheological properties could be easily obtained. Additionally, it was suggested the biological action of unknown compounds. Thus, we believe that new insights could be provided regarding the interaction of cytotoxic Isovanillin derivatives with components of cell membranes since parameters related to intermolecular interactions and their effects on the thermodynamic and rheological properties can be easily obtained and related to the biological action of membrane active compounds. Thus, these facts are therefore relevant in order to understand the biophysical aspects involved in the interaction of natural products and its derivatives with cellular membranes in many of these actions as an anticancer agents.

Acknowledgements

The authors thank the financial support from Fundação de Amparo a Pesquisa do Estado de São Paulo (FAPESP, process 2010/51313-0) and CAPES - Finance Code 001 (Coordenação de Aperfeiçoamento de Pessoal de Nível Superior) for the scholarship granted to ACC.

References

- [1] F.V. Nussbaum, M. Brands, B. Hinz, S. Weigand, D.H. Bich, Antibacterial natural products in medicinal chemistry - exodus or revival? *Angew. Chem. Int. Ed.* 45 (2006) 5072–5129.
- [2] J. Chen, W. Li, H. Yao, J. Xu, Insights into drug discovery from natural products through structural modification, *Fitoterapia* 103 (2015) 231–241.
- [3] H. Yao, J. Liu, S. Xu, Z. Zhu, J. Xu, The structural modification of natural products for novel drug discovery, *Expert Opin. Drug Discov.* 12 (2017) 121–140.
- [4] J.M. Liu, M.Y. Ni, J.F. Fan, Y.Y. Tu, Z.H. Wu, Y.L. Wu, Structure and reaction of arteannuin, *Acta Chim. Sin.* 37 (1979) 129–141.
- [5] Z. Guo, Artemisinin anti-malarial drugs in China, *Acta Pharm. Sin. B* 6 (2016) 115–124.
- [6] S. Zhu, W. Liu, X. Ke, J. Li, R. Hu, H. Cui, G. Song, Artemisinin reduces cell proliferation and induces apoptosis in neuroblastoma, *Oncol. Rep.* 32 (2014) 1094–1100.
- [7] R. He, B.T. Mott, A.S. Rosenthal, D.T. Genna, G.H. Posner, R. Arav-Boger, An artemisinin-derived dimer has highly potent anti-cytomegalovirus (CMV) and anti-cancer activities, *PLoS ONE* 6 (2011) 6–11.
- [8] A.J. Lin, D.I. Klayman, W.K. Milhous, Antimalarial activity of new water-soluble dihydroartemisinin derivatives, *J. Med. Chem.* 30 (1987) 2147–2150.
- [9] R.K. Haynes, B. Fugmann, J. Stetter, K. Rieckmann, H.D. Heilmann, H.W. Chan, M.K. Cheung, W.L. Lam, H.N. Wong, S.L. Croft, L. Vivas, L. Rattray, L. Stewart, W. Peters, B.L. Robinson, M.D. Edstein, B. Kotecka, D.E. Kyle, B. Beckermann, M. Gerisch, M. Radtke, G. Schmuck, W. Steinke, U. Wollborn, K. Schmeer, A. Romer, Artemisone - A highly active antimalarial drug of the artemisinin class, *Angew. Chem. Int. Ed.* 45 (2006) 2082–2088.
- [10] J. Chen, L. Wenlong, Y. Hequan, Insights into drug discovery from natural products through structural modification, *Fitoterapia* 103 (2015) 231–241.
- [11] J. Zhang, L. Wang, H. Li, C. Zhuang, T. Mizuno, H. Ito, C. Suzuki, H. Okamoto, J. Li, Antitumor polysaccharides from a Chinese Mushroom, “Yuhuangmo” the fruiting body of *Pleurotus citrinopileatus*, *Biosci. Biotech. Biochem.* 58 (1994) 1195–1201.
- [12] C.Y. Li, E.Q. Wang, Y. Cheng, J.K. Bao, Oridonin: an active diterpenoid targeting cell cycle arrest, apoptotic and autophagic pathways for cancer therapeutics, *Int. J. Biochem. Cell Biol.* 43 (2011) 701–704.
- [13] S. Xu, Dahong Li, L. Pei, H. Yao, C. Wang, H. Cai, H. Yao, X. Wu, J. Xu, Design synthesis and antimycobacterial activity evaluation of natural oridonin derivatives, *Bioorganic Med. Chem. Lett.* 24 (2014) 2811–2814.
- [14] H. Tsuchiya, Membrane interactions of phytochemicals as their molecular mechanism applicable to the discovery of drug leads from plants, *Molecules* 20 (2015) 18923–18966.
- [15] J.V. Ferreira, T.M. Capello, L.J.A. Siqueira, J.H.G. Lago, L. Caseli, Mechanism of action of thymol on cell membranes investigated through lipid langmuir monolayers at the air–water interface and molecular simulation, *Langmuir* 32 (2016) 3234–3241.
- [16] H. Brockman, Lipid monolayers: why use half a membrane to characterize protein-membrane interactions? *Curr. Opin. Struct. Biol.* 9 (1999) 438–443.
- [17] B. Korchowiec, M. Gorczyca, K. Wojszko, M. Janikowska, M. Henry, E. Rogalska, Impact of two different saponins on the organization of model lipid membranes, *Biochim. Biophys. Acta – Biomembr.* 1848 (2015) 1963–1973.
- [18] M. Flasiński, K. HaC-Wydro, M. Broniatowski, Incorporation of pentacyclic triterpenes into mitochondrial membrane - studies on the interactions in model 2D lipid systems, *J. Phys. Chem. B* 118 (2014) 12927–12937.
- [19] R.M. Wilson, S.J. Danishefsky, Small molecule natural products in the discovery of therapeutic agents: the synthesis connection, *J. Organic Chem.* 71 (2006) 8329–8351.
- [20] A.C. Carvalho, João C.S. Lira, T.M. Pereira, S.C. Silva, S.Y. Simote-Silva, F.K.D. Oliveira, B. King-Diaz, B. Lotina-Hennsen, T.A.M. Veiga, Natural products from *Pluchea sagittalis* act as inhibitors of photosynthesis *in vitro*, *Nat. Prod. Res.* 6419 (2017) 1–6.
- [21] H. Sadraei, M. Ghanadian, G. Asghari, E. Madadi, Antispasmodic activity of isovanillin and isoacetovanillin in comparison with *Pycnocycla spinosa* Decne. extract on rat ileum, *Res. Pharm. Sci.* 9 (2014) 187–192.
- [22] D. Begum, S.C. Nath, Ethnobotanical review of medicinal plants used for skin diseases and related problems in Northeastern India, *J. Herbs Spices Med. Plants* 6475 (2008) 37–41.
- [23] J. Liu, P. Li, Q. Wang, B. Li, G. Li, The HPLC fingerprint and isovanillin content of *Benincasa hispida* seeds, *J. Chem.* 2015 (2015).
- [24] C. Cole, T. Burgoyne, A. Lee, L. Stehno-Bittel, G. Zaid, Arum Palaestinum with isovanillin, linolenic acid and β -sitosterol inhibits prostate cancer spheroids and reduces the growth rate of prostate tumors in mice, *BMC Compl. Altern. Med.* 15 (2015) 1–8.
- [25] A.J. Al-Rehaily, M.H.M. Sharaf, M.A. Zemaitis, C.Y. Gao, G.E. Martin, C.E. Hadden, T.J. Thamann, F.T. Lin, P.L. Schiff, Thalprzewalskiinone, a new oxobenzylisoquinoline alkaloid from *Thalictrum przewalskii*, *J. Nat. Prod.* 62 (1999) 146–148.
- [26] G.A. Dunne, S. Prendergast, D. Telford, Short report, *Health* 4 (2010) 103–115.
- [27] K. Lirdprapamongkol, H. Sakurai, N. Kawasaki, M.K. Choo, Y. Saitoh, Y. Aozuka, P. Singhirunnusorn, S. Ruchirawat, J. Svasti, I. Saiki, Vanillin suppresses *in vitro* invasion and *in vivo* metastasis of mouse breast cancer cells, *Eur. J. Pharm. Sci.* 25 (2005) 57–65.
- [28] K. Lirdprapamongkol, H. Sakurai, S. Suzuki, K. Koizumi, O. Prangsaengtong, A. Viriyaroj, S. Ruchirawat, J. Svasti, I. Saiki, Vanillin enhances TRAIL-induced apoptosis in cancer cells through inhibition of NF-kappaB activation, *In vivo* (Athens, Greece) 24 (2010) 501–506.
- [29] J. Deb, H. Dibra, S. Shan, S. Rajan, J. Manneh, C.S. Kankipati, C.J. Perry, I.D. Nicholl, Activity of aspirin analogues and vanillin in a human colorectal cancer cell line, *Oncol. Rep.* 26 (2011) 557–565.
- [30] G.V.M. Sharma, A. Ramesh, A. Singh, G. Srikanth, V. Jayaram, D. Duscharla, J.H. Jun, R. Ummanni, S.V. Malhotra, Imidazole derivatives show anticancer potential by inducing apoptosis and cellular senescence, *Med. Chem. Comm.* 5 (2014) 1751–1760.
- [31] Y.Q. Yan, Q.Z. Xu, L. Wang, J.L. Sui, B. Bai, P.K. Zhou, Vanillin derivative 6-bromine-5-hydroxy-4-methoxybenzaldehyde-elicited apoptosis and G2/M arrest of Jurkat cells proceeds concurrently with DNA-PKcs cleavage and Akt inactivation, *Int. J. Oncol.* 29 (2006) 1167–1172.
- [32] L.F.G. Salis, G.N. Jaroque, J.F.B. Escobar, C. Giordani, A.M. Martinez, D.M.M. Fernández, F. Castelli, M.G. Sarpietro, L. Caseli, Interaction of 3',4',6'-trimyristoyl-uridine derivative as potential anticancer drug with phospholipids of tumorigenic and non-tumorigenic cells, *Appl. Surf. Sci.* 426 (2017) 77–86.
- [33] J.A.F. Op Den Kamp, Lipid asymmetry in membranes, *Ann. Rev. Biochem.* 48 (1979) 47–71.
- [34] P.B. Alves, M.M. Victor, Reação da cânfora com borodireto de sódio: Uma estratégia para o estudo da estereoquímica da reação de redução, *Quim. Nova* 33 (2010) 2274–2278.
- [35] J.G. Riley, C. Xu, I. Brockhausen, Synthesis of acceptor substrate analogs for the study of glycosyltransferases involved in the second step of the biosynthesis of O-antigen repeating units, *Carbohydr. Res.* 345 (2010) 586–597.
- [36] Y. Liang, C. Yan, N.F. Schor, Apoptosis in the absence of caspase 3, *Oncogene* 20 (2001) 6570–6578.
- [37] G.S. Salvesen, V.M. Dixit, Caspases: intracellular signaling by proteolysis, *Cell* 91 (1997) 443–446.
- [38] S. Dasari, P.B. Tchounwou, Cisplatin in cancer therapy: molecular mechanisms of action, *Eur. J. Pharmacol.* 740 (2015) 364–378.
- [39] M. Broniatowski, P. Mastalerz, M. Flasiński, Studies of the interactions of ursane-type bioactive terpenes with the model of *Escherichia coli* inner membrane—Langmuir monolayer approach, *Biochim. Biophys. Acta* 1848 (2014) 469–476.
- [40] G.E.G. Gonçalves, F.S. Souza, J.H.G. Lago, L. Caseli, The interaction of eugenol with cell membrane models at the air–water interface is modulated by the lipid monolayer composition, *Biophys. Chem.* 207 (2015) 7–12.

Glossary

B16F10-Nex2: murine melanoma cell line

HL-60: human leukemia cell line

MCF-7: human breast adenocarcinoma cell line

A2058: human melanoma cell line

HeLa: human epitheloid cervix carcinoma cell line

DPPC: 1,2-dipalmitoyl-*sn*-glycero-3-phosphocoline

DPPS: 1,2-dipalmitoyl-*sn*-glycero-3-phosphoserine

MTT: 3-[4,5-dimethylthiazol-2-yl]-2,5-diphenyltetrazolium bromide

LE: liquid-expanded phase

LC: liquid-condensed phase